

Supporting Information for the article:

Sustainable Catalysts in a Short Time: Harnessing Bacteria for Swift Palladium Nanoparticle Production

Olga A. Kamanina^a, Pavel V. Rybochkin^a, Daria V. Borzova^a, Vitaliy N. Soromotin^a, Alexey S. Galushko^b, Alexey S. Kashin^b, Anton N. Zvonarev^c, Nina M. Ivanova^b, Natalia E. Suzina^c, Angelina A. Holicheva^a, Daniil A. Boiko^b, Vyacheslav A. Arlyapov^a, Valentine P. Ananikov^{*b,d}

^a*Tula State University, Pr. Lenina 92, Tula 300012, Russia*

^b*Zelinsky Institute of Organic Chemistry, Russian Academy of Sciences, Leninsky Pr. 47, Moscow 119991, Russia;*

^c*Federal Research Center “Pushchino Scientific Center for Biological Research of the Russian Academy of Sciences”, Skryabin Institute of Biochemistry and Physiology of Microorganisms, 142290 Pushchino, Russia*

^d*Organic Chemistry Department, RUDN University, 6 Miklukho-Maklaya St, Moscow, 117198, Russia*

E-mail: val@ioc.ac.ru; <https://AnanikovLab.ru>

Table of contents

Materials and methods	S2
Bacterial cell cultivation	S2
Preparation of Pd/P. <i>yeei</i> with various durations of hydrogen flow	S2
Scanning electron microscopy (SEM)	S3
Scanning transmission electron microscopy (STEM) of catalyst sections	S3
TEM Measurements.....	S3
Fluorescence microscopy of bacterial cells	S3
The arylation of styrene (the Mizoroki–Heck reaction)	S3
Heat-killed cells. Enzyme activity analysis	S3
Detection of nanoparticles on STEM images	S4
Additional SEM and fluorescence microscopy data.....	S5
Nanoparticle size analysis before and after drying.....	S6
Examples of nanoparticle detection on STEM images	S7
Nanoparticle size distribution by covered area analysis	S8
Additional ¹ H NMR spectra of products	S9
XPS analysis of Pd/P. <i>yeei</i>	S10
Blank test (role of hydrogen purge).....	S10
References.....	S11

Materials and methods

NMR spectra were recorded using a Bruker AVANCE DRX 500 spectrometer at a frequency of 500.13 MHz (^1H), with the residual solvent peak used as an internal standard. The spectra were processed using MestReNova software. Gas chromatography–mass spectrometry (GC–MS) studies were performed on a Maestro- α quadrupole instrument using an electron ionization (EI–MS) source with sample injection via a CrystalLux-4000 M gas chromatograph. The ionization energy was set to 70 eV.

In this work, the following substances were used: peptone (Molekula Ltd., UK), yeast extract (Bio Springer, France), agar (Bio-Rad, France), NaCl ($\geq 99\%$, Helicon, Russia), styrene (Sigma–Aldrich, USA), K_2CO_3 (ABCR GmbH & Co. KG, Germany), dimethylformamide (Sigma–Aldrich, USA), acetonitrile (Komponent-reaktive, Russia), 1-bromo-4-nitrobenzene (Sigma–Aldrich, USA), Pd/C 5 wt. % (ACROS Organics, Belgium, №195020100), palladium acetate (Fluorochem, UK), deuterated chloroform (Carl Roth GmbH & Co. KG, Germany).

Bacterial cell cultivation

The bacterial strain *Paracoccus yeei* VKM B-3302 was isolated by the research team of the authors from activated sludge derived from municipal wastewater treatment plants ¹. The *Paracoccus yeei* bacteria are obligate aerobes. Gram-negative cocci with a small cell diameter (approximately 0.5–0.9 μm), which enables the production of a high palladium nanoparticle content per unit mass of the bacterial support in the resulting catalyst. They exhibit a high growth rate, ease of propagation and maintenance in pure culture ². Another notable feature of these microorganisms is their resistance to metal salts ^{3,4}, which allows the formation of nanoparticles in systems with a living bacterial support. Cultivation was performed on Luria–Bertani (LB) nutrient media supplemented with 10 g/l peptone, 10 g/l NaCl and 5 g/l yeast extract. The bacterial cells cultivated in 750 cm^3 Erlenmeyer flasks with a nutrient medium volume of 200 cm^3 at a temperature of 28 $^\circ\text{C}$ while aerated in a shaker at 180 rpm. After 48 hours, the bacterial culture was harvested by centrifugation at 8000 rpm for 10 minutes in test tubes. The cell biomass was dried and then stored in test tubes at +4 $^\circ\text{C}$.

Preparation of Pd/*P. yeei* with various durations of hydrogen flow

The general preparation procedure for Pd/*P. yeei* 4.4 wt. % was described in our previous study ⁵. A mixture of bacterial cells with palladium acetate (Figure S1A) was prepared in distilled water. Argon was applied for 0.5 minutes. The mixture was shaken for 10 minutes (180 rpm; 28 $^\circ\text{C}$) (Figure S1B). Then, hydrogen was sparged through the mixture for a defined time (0.5, 1, 2, 3, 5 and 10 min) to reduce Pd(II) to Pd(0) (Figure S1C). The biomass of bacterial cells with Pd nanoparticles (Figure S1D) was harvested via centrifugation (12000 rpm, 10 min using a BKC-TH16D centrifuge) in test tubes (Figure S1E). The sediment of the Pd/*P. yeei* was separated and dried at room temperature for at least 2 days (Figure S1F). The average Pd content of the Pd/*P. yeei* catalyst after preparation was found to be 4.4 ± 0.5 wt% by inductively coupled plasma mass spectrometry.



Figure S1. Preparation procedure for Pd/*P. yeei* catalyst: A – mixture of bacterial cells with palladium acetate, B – 10 minutes of shaking, C – reduction of Pd(II) to Pd(0), D – mixture of cells with Pd nanoparticles, E – harvested catalyst in test tubes, F – dried Pd/*P. yeei* catalyst

The blank test was carried out as described above with one exception. Hydrogen was changed to atmospheric air in purge.

Scanning electron microscopy (SEM)

Double-sided carbon tape was attached to a standard 1-inch diameter aluminum specimen stub. The synthesized and dried Pd/P. *yei* materials were placed on the surface of double-sided carbon tape. The prepared samples were dried under vacuum (10^{-4} mbar, 5 min) and covered with a 15 nm film of carbon using a Cressington 208 carbon coater. SEM observations were carried out with a Hitachi Regulus 8230 (SU8230) field-emission scanning electron microscope. Images were acquired in backscattered electron mode (compositional contrast) at an accelerating voltage of 10 kV.

Scanning transmission electron microscopy (STEM) of catalyst sections

The freshly synthesized Pd/P. *yei* catalyst sample was sectioned with an ultramicrotome according to the following method. To prepare ultrathin sections, Pd/P. *yei* biohybrid was fixed in 2 % glutaraldehyde solution in 0.05 M cacodylate buffer (pH 7.2) for 1 h at 4 °C. The sample was subsequently washed three times with 0.05 M cacodylate buffer (pH 7.2). The dehydrated sample in the agar blocks was subsequently encapsulated in Epon 812 epoxy resin and then sectioned using a Reichert-Jung UltraCut E ultramicrotome. STEM observations were carried out with a Hitachi Regulus 8230 (SU8230) field-emission scanning electron microscope. Images were acquired in bright-field STEM mode at an accelerating voltage of 30 kV.

TEM Measurements

Bacterial cells sections prepared as described above were studied using Hitachi HT7700 transmission electron microscope. Images were acquired in bright-field TEM mode at an accelerating voltage of 100 kV. The nanoparticle size distribution was determined via ImageJ software and the DLgram cloud service for deep-learning analysis of microscopy images⁶.

Fluorescence microscopy of bacterial cells

A LIVE/DEAD™ BacLight™ Bacterial Viability Kit (Molecular Probes) was used to detect live and dead cells. One microliter of the appropriate dye from the kit was added to 0.5 ml of microbial suspension. The samples were examined via fluorescence microscopy on an AXIO Imager A1 instrument (Zeiss) with a 56HE filter set (Zeiss) at 470 nm (excitation) and 512 nm+630 nm (emission). Image acquisition was performed via an AxioCam 506 camera (Zeiss).

The arylation of styrene (the Mizoroki–Heck reaction)

A 1 mol. % catalyst (Pd/P. *yei* 4.4wt.% obtained with various hydrogen purge durations or Pd/C 5wt.% or Pd/P. *yei* 4.4wt% from blank test) was mixed with other solid reagents (101 mg, 0.5 mmol. 1-bromo-4-nitrobenzene; 69.1 mg, 0.5 mmol. K_2CO_3) in the test tube equipped with a magnetic stirrer bar. The solvent (2.5 cm³ dimethylformamide) and styrene (0.5 mmol; 0.0575 cm³) were added to the solid reagents. The reaction mixture was stirred and heated for 5 hours (140 °C; 1200 rpm).

After 5 h, samples were taken from the reaction mixture for GC-MS and NMR analysis. The sample for GC-MS (0.01 cm³) was subsequently diluted 10^4 times with acetonitrile before analysis. The deuterated solvent (0.5 cm³) was added to the NMR sample (0.1 cm³) prior to measurements and obtained ¹H NMR spectra.

Heat-killed cells. Enzyme activity analysis

Three suspensions of cells were prepared in distilled water. The first mixture was autoclaved for 45 minutes (1.1 atm; 121 °C). The second mixture was heated at 60 °C for 30 minutes (pasteurization). The third mixture was used as a control without pretreatment. Nonspecific dehydrogenase activity was determined by adding a weak solution of methylene blue to medium supplemented with glucose and pretreated cells. Methylene blue acts as a hydrogen acceptor, intercepting it from dehydrogenase; thus, the oxidized form of methylene

blue becomes a reduced and colorless leukoform. The cuvette was filled with oil after the introduction of methylene blue to prevent the restoration of color by air-oxygen oxidation. The disappearance of color was determined via a spectrophotometer (SF 2000) in kinetic mode at a specific wavelength.

Detection of nanoparticles on STEM images

The nanoparticles detection was performed using OpenCV library ⁷ in two steps: obtaining a map of approximate nanoparticle locations and subsequently searching for nanoparticle contours filtered by size. For the first stage, the following operations were applied:

1) Adaptive thresholding with gaussian adaptive method for threshold value calculation. The block size was equal to 41, and the constant C was equal to 7 for images at 100k magnification (and more) and to 12 for images at 20k or 50k magnification. This method of binarization was selected because it yields better results for images with varying illuminations and high contrast.

2) Morphological transformations include dilation with a (5, 5) kernel and erosion with a (3, 3) kernel to reduce noise in the binarized image.

3) Median blurring filter with (5, 5) kernel for additional image smoothing.

Notably, binarization of images with different magnifications was implemented in various ways. If the image had 100k magnification or more, the method was applied to the whole image. Otherwise, if 20k or 50k magnification was used, the procedure was performed for each of eight crops of the image that were previously upscaled 3 times via bicubic interpolation.

In the second step, contour search was implemented. For each contour, a convex hull was found, and if the contour area was less than 70% of its area, the corresponding contour was replaced by the convex hull.

Then, for each contour, a minimal enclosing circle, a diameter in nanometers and coordinates of the center have been found. This information was used for contour filtering by linear size. The results of this stage form two arrays: the contour array and the nanoparticle array, which contain data about nanoparticle location and size.

Finally, the detection of nanoparticles on cells and in the surrounding solution was performed. For this purpose, cell segmentation was performed using Cellpose3 algorithm ⁸ (the “cyto3” model). Then, the obtained segmentation masks were used to determine the nanoparticles on the cells and the free nanoparticles: the center of the nanoparticle was checked for belonging to the area with cells.

Additional SEM and fluorescence microscopy data

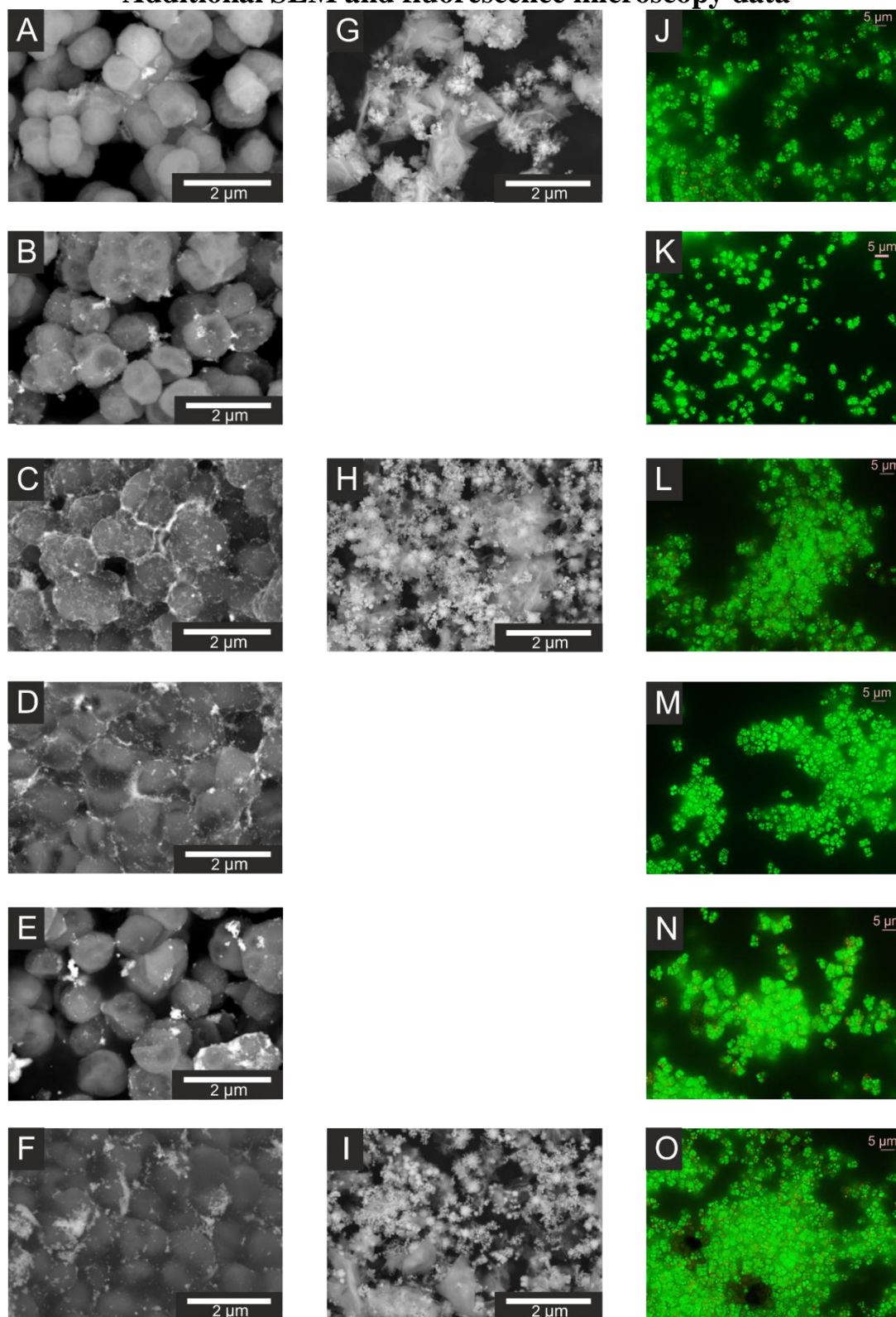


Figure S2. SEM images of cells and the Pd(OAc)₂ system after different H₂ purge times: A – 30 s; B – 1 min; C – 2 min; D – 3 min; E – 5 min; F – 10 min; SEM images of Pd(OAc)₂ without microorganisms after different H₂ purge times: G – 30 s; H – 2 min; I – 10 min; fluorescence microscopy images of the bacteria and Pd(OAc)₂ system: J – microorganisms without hydrogen purge; K – after 30 s of hydrogen purge; L – after 1 min of hydrogen purge; M – after 3 min of hydrogen purge; N – after 5 min of hydrogen purge; O – after 10 min of hydrogen purge.

Nanoparticle size analysis before and after drying

Air-drying the samples does not cause nanoparticle agglomeration. This was confirmed by ultrathin section microscopy See Figure S3 for photographs and particle distributions.

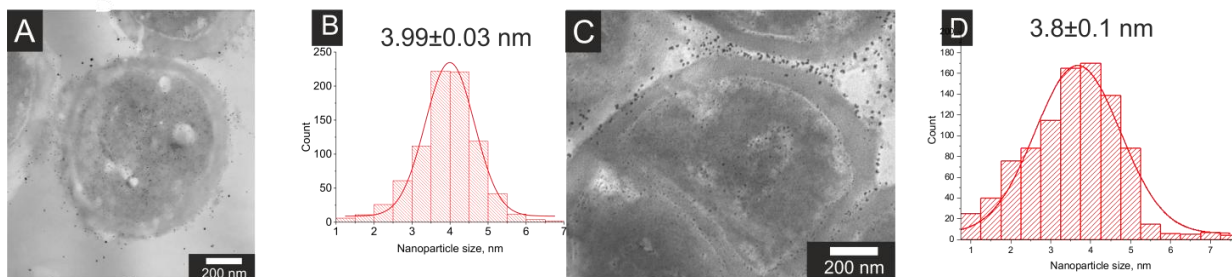


Figure S3. STEM images of Pd/*P. yeii* catalyst: A – before air-drying; C – after air-drying. Nanoparticle size distribution in catalyst: B – before air-drying, D – after air-drying

Examples of nanoparticle detection on STEM images

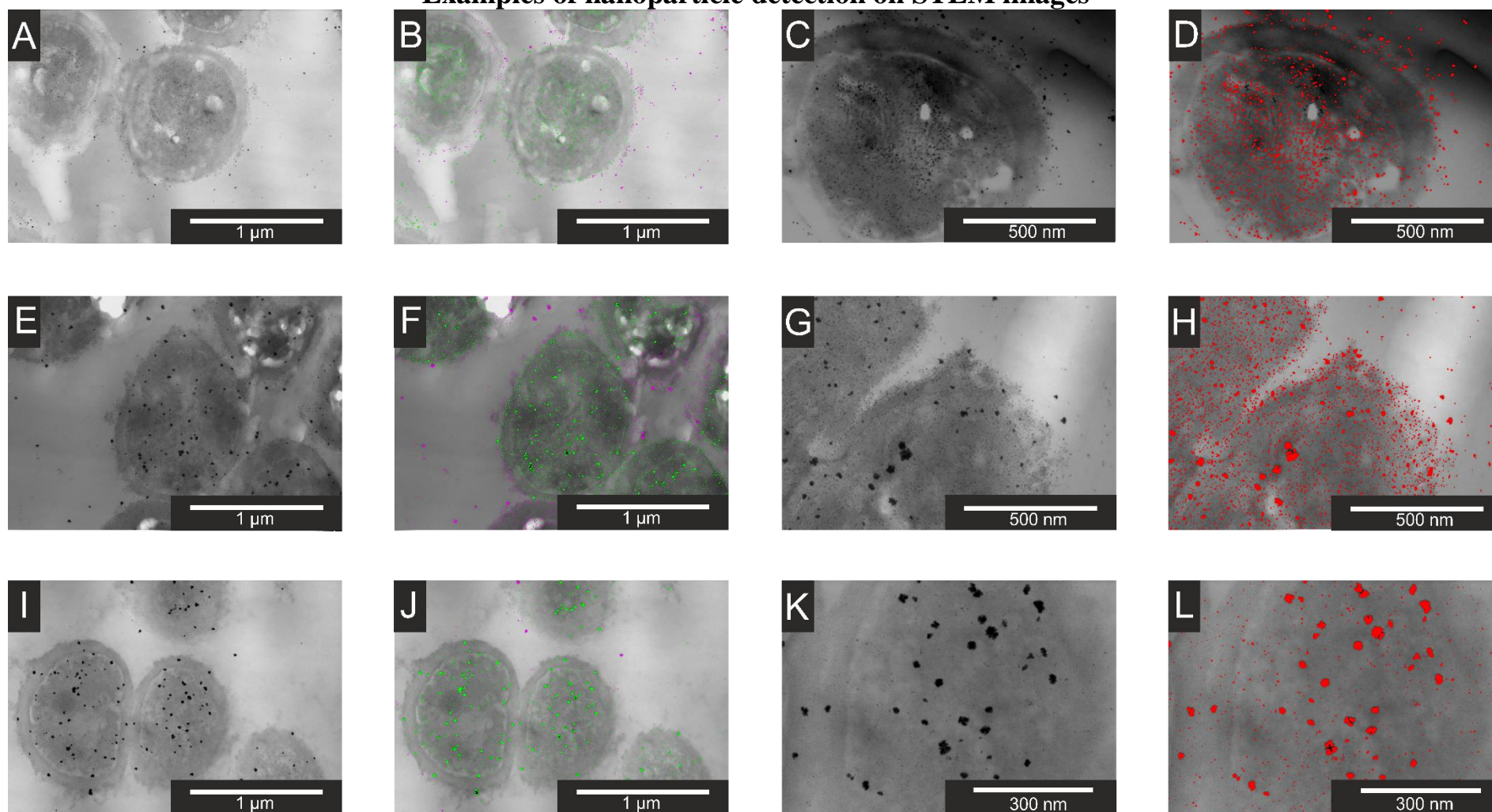


Figure S4. STEM images of detected nanoparticles in Pd/*P. yeii* catalyst prepared with: A, B, C, D – living; E, F, G, H – pasteurized; I, J, K, L – autoclaved. For images with multiple bacterial cells, the green areas correspond to Pd NPs inside microorganisms, and the magenta areas correspond to Pd NPs outside microorganisms. The red areas highlight all nanoparticles in the image.

Nanoparticle size distribution by covered area analysis

The STEM images of the hybrid biocatalyst sections obtained after 2 minutes of hydrogen flow clearly revealed palladium nanoparticles both outside and inside the microorganisms (Figure S5 A, C, E). The intra- and extracellular size distributions of the nanoparticles were calculated as a function of the area occupied by these particles. For the catalyst prepared from live *P. yeii* cells, the average size of the Pd NPs was 5.6 nm (Figure S5 B). In contrast, the use of pasteurized cells in catalyst preparation resulted in an average size of NPs of 14.8 nm (Figure S5 D), whereas the use of autoclaved cells resulted in an even more pronounced increase in the average NPs size to 21.2 nm (Figure S5 F).

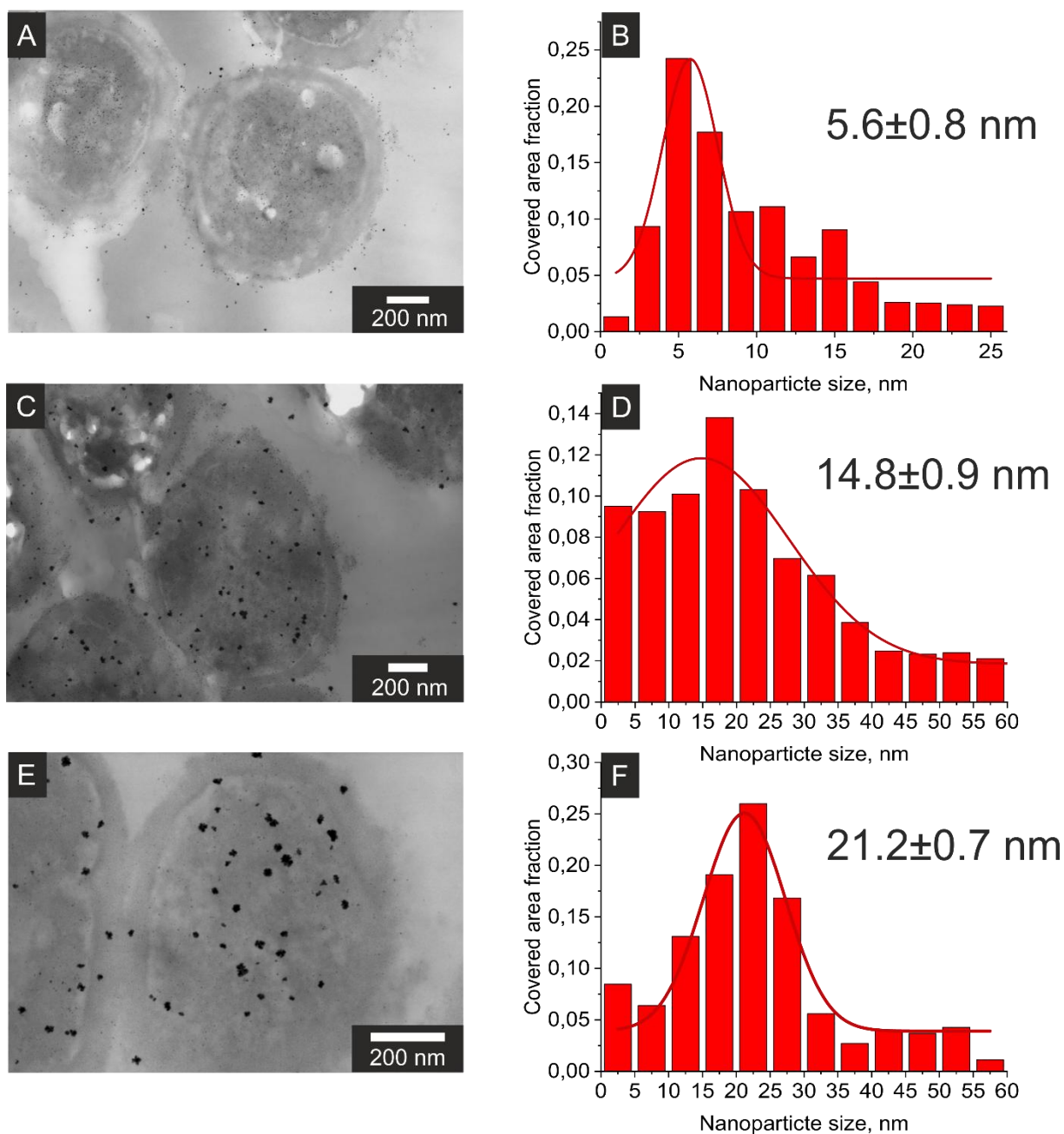


Figure S5. STEM images of Pd/*P. yeii* catalyst at $\times 50k$ magnification prepared with *P. yeii*: A – living; C – pasteurized; E – autoclaved and corresponding particle size distribution patterns B, D, F.

Additional ^1H NMR spectra of products

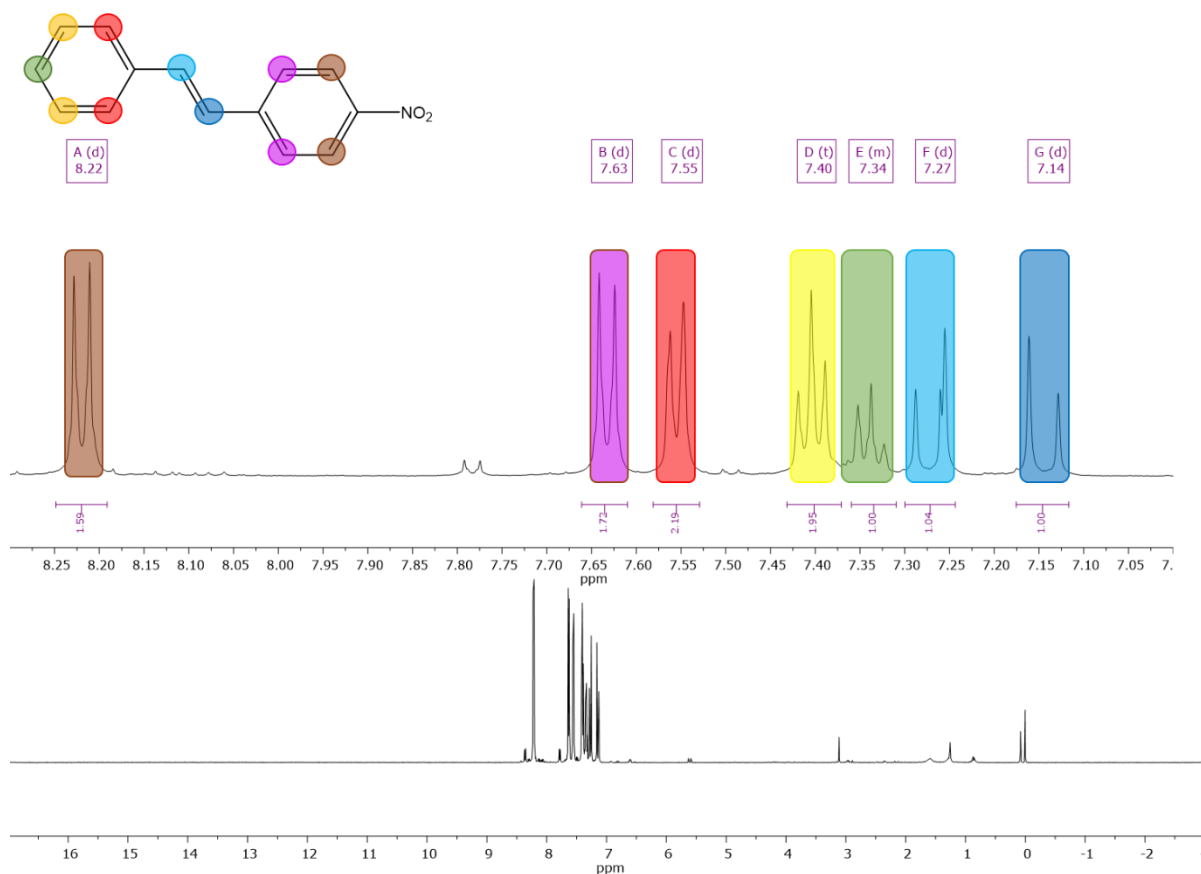


Figure S6. ^1H NMR spectra of crude product obtained using Pd/*P. yeei*

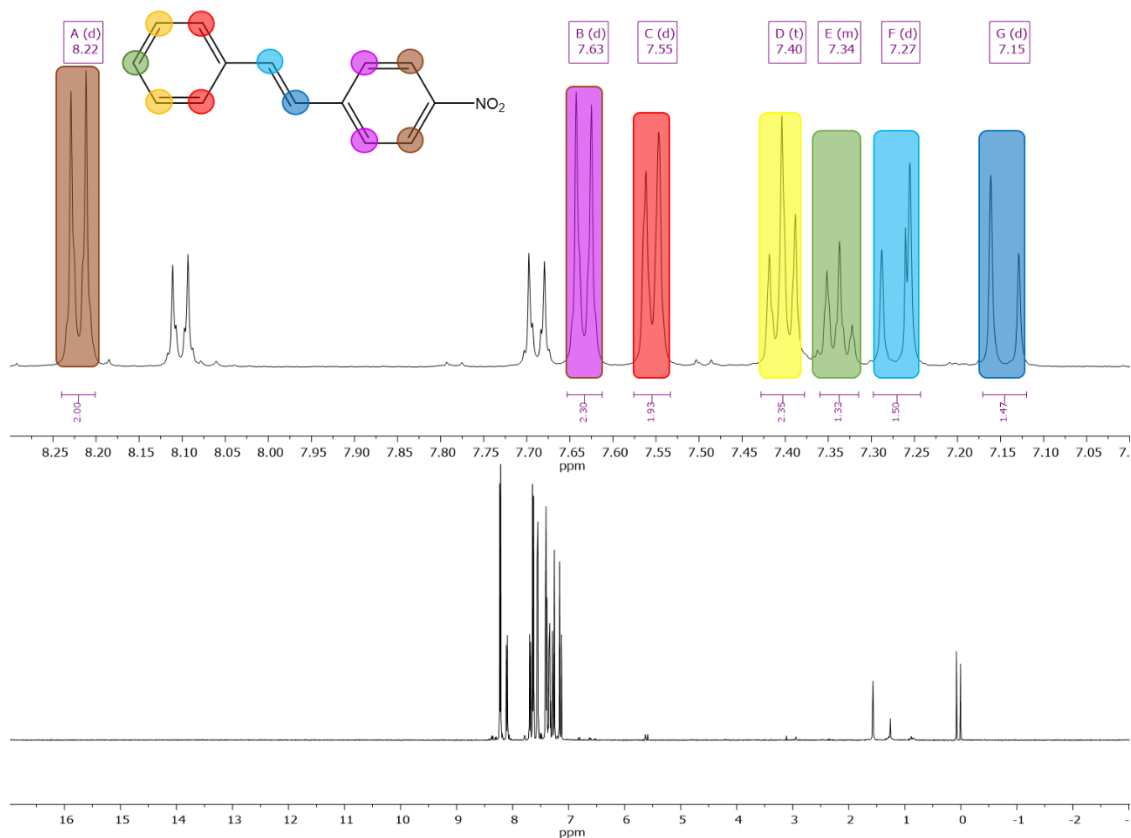


Figure S7. ^1H NMR spectra of crude product obtained using Pd/C

Figure S6. ^1H NMR (500 MHz, Chloroform-*d*) δ 8.22 (d, J = 8.8 Hz, 2H), 7.63 (d, J = 8.8 Hz, 2H), 7.55 (d, J = 7.4 Hz, 2H), 7.40 (t, J = 7.6 Hz, 2H), 7.36 – 7.31 (m, 1H), 7.27 (d, J = 16.3 Hz, 1H), 7.14 (d, J = 16.3 Hz, 1H).

Figure S7. ^1H NMR (500 MHz, Chloroform-*d*) δ 8.22 (d, J = 8.9 Hz, 2H), 7.63 (d, J = 8.8 Hz, 2H), 7.55 (d, J = 7.7 Hz, 2H), 7.40 (t, J = 7.5 Hz, 2H), 7.36 – 7.31 (m, 1H), 7.27 (d, J = 16.3 Hz, 1H), 7.15 (d, J = 16.3 Hz, 1H).

Peaks at δ 8.10 (d, J = 9.0 Hz, 2H) and δ 7.69 (d, J = 9.0 Hz, 2H) correspond to protons in initial 1-bromo-4-nitrobenzene

Spectra of product corresponds to ⁹ and ¹⁰.

XPS analysis of Pd/*P. yeii*

Studies by XPS were carried out on an OMICRON ESCA+ spectrometer with an aluminum anode equipped with a monochromatic X-ray source Al K α XM1000 (with a radiation energy of 1486.6 eV and a power of 252 W). Registration of the spectra was carried out by a hemispherical detector-analyzer Argus. To eliminate the local charge on the analyzed surface, a CN-10 charge neutralizer with an emission current of 4 μA and a beam energy of 1 eV was used. The transmission energy of the analyzer was 20 eV. The spectrometer was calibrated along the Au4f 7/2 line at 84.1 eV. The pressure in the analyzer chamber did not exceed 10^{-9} mbar. All spectra were accumulated at least three times. The peak position fluctuation did not exceed ± 0.1 eV.

Blank test (role of hydrogen purge)

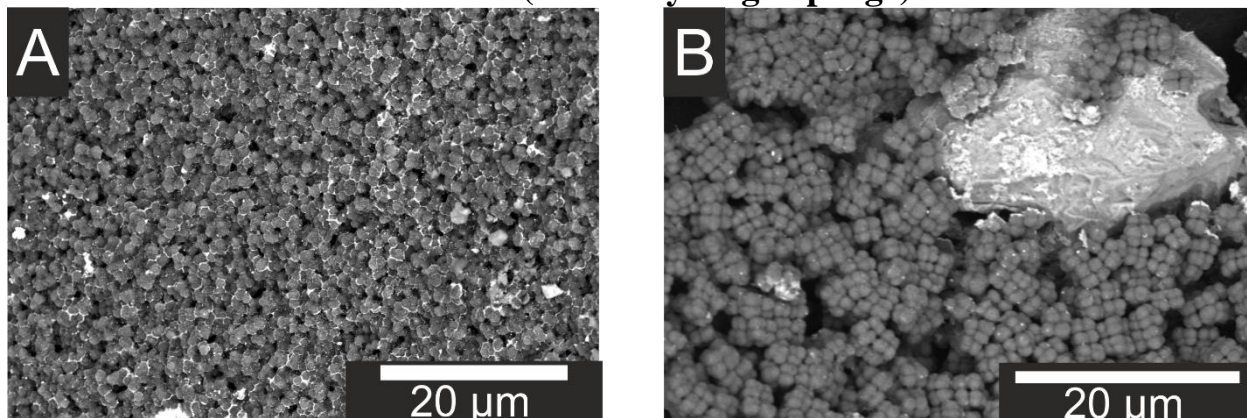


Figure S8. SEM images for Pd/*P. yeii* catalyst prepared using: A –hydrogen purge (typical catalyst preparation procedure); B – air purge (blank experiment)

Atmospheric air purging resulted in minimal metal coating of the bacteria and the presence of the original palladium salt was observed (Figure S8B). The yield of the Mizoroki-Heck reaction was approximately 5% with the catalyst from the blank test, confirming ineffective nanoparticle formation. Thus, hydrogen purge was required for effective Pd/*P. yeii* preparation.

References

1. A. S. Kharkova, V. A. Arlyapov, A. D. Turovskaya, A. N. Avtukh, I. P. Starodumova and A. N. Reshetilov, *Appl. Biochem. Microbiol.*, 2019, **55**, 189-197.
2. V. A. Arlyapov, N. Y. Yudina, L. D. Asulyan, O. A. Kamanina, S. V. Alferov, A. N. Shumsky, A. V. Machulin, V. A. Alferov and A. N. Reshetilov, *3 Biotech*, 2020, **10**, 207.
3. A. S. Kharkova, V. A. Arlyapov, A. D. Turovskaya, V. I. Shvets and A. N. Reshetilov, *Enzyme Microb. Technol.*, 2020, **132**, 109435.
4. O. Kamanina, V. Arlyapov, P. Rybochkin, D. Lavrova, E. Podsevalova and O. Ponamoreva, *3 Biotech*, 2021, **11**, 331.
5. P. V. Rybochkin, R. N. Perchikov, B. Y. Karlinskii, O. A. Kamanina, V. A. Arlyapov, A. S. Kashin and V. P. Ananikov, *J. Catal.*, 2024, **429**, 115238.
6. A. V. Matveev, A. V. Nartova, N. N. Sankova and A. G. Okunev, *Microsc. Res. Tech.*, 2024, **87**, 991-998.
7. G. Bradski, *The OpenCV Library. Dr Dobb's J Softw Tools*, 2000, **25**, 120-125.
8. C. Stringer and M. Pachitariu, *bioRxiv*, 2024, 2024.2002. 2010.579780.
9. A. Banik and S. K. Mandal, *ACS Catal.*, 2022, **12**, 5000-5012.
10. Q. Yao, M. Zabawa, J. Woo and C. Zheng, *J. Am. Chem. Soc.*, 2007, **129**, 3088-3089.